

Near IR Photolysis of HO₂NO₂: Implications for HO_x

Ross J. Salawitch¹, Paul O. Wennberg², Geoffrey C. Toon¹, Bhaswar Sen¹, and Jean-Francois Blavier¹

¹Jet Propulsion Laboratory, California Institute of Technology, Pasadena, CA

²California Institute of Technology, Pasadena, CA

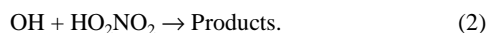
Abstract. We report observations and calculations of peroxyoxynitric acid, HO₂NO₂, in the stratosphere and upper troposphere. The simulations show that photolysis of HO₂NO₂ via excitation of purely vibrational modes at wavelengths longward of 760 nm (the near IR) can dominate loss of this species. Consideration of this photolytic pathway reduces calculated HO₂NO₂, resolving a large discrepancy between standard model calculations and observations of HO₂NO₂ at high-latitude spring. The lower calculated abundance of HO₂NO₂ reduces the efficiency of the OH+HO₂NO₂ sink of HO_x. Consideration of this process leads to large increases in calculated HO_x (20 to 60%) for high-latitude spring and better agreement with observed stratospheric abundances of HO_x. Near IR photolysis of HO₂NO₂ alters the coupling between NO_x and HO_x in stratospheric and upper tropospheric photochemical models.

1. Introduction

Peroxyoxynitric acid, HO₂NO₂, is important to the photochemistry of the upper troposphere and stratosphere. It is formed by:



and removed by photolysis as well as reaction with OH:



Assuming reaction (2) produces H₂O and O₂, the sequence (1) + (2) catalyzes the loss of HO_x (e.g., OH + HO₂ → H₂O + O₂).

The first measurements of HO₂NO₂ were based on spectra obtained by the Atmospheric Trace Molecule Spectroscopy experiment [Rinsland *et al.*, 1986]. Subsequent laboratory measurements of HO₂NO₂ line parameters [May and Friedl, 1993] improved the precision of these and other remote observations of HO₂NO₂ [e.g., Sen *et al.*, 1998]. Previous studies focused on profiles obtained at mid-latitudes, where the discrepancy between modeled and measured HO₂NO₂ is small [Sen *et al.*, 1998], well within the range of model uncertainty.

Recently, new measurements of photodissociation cross sections of HO₂NO₂ have been reported for both the UV [Knight *et al.*, 2002] and the near IR [Roehl *et al.*, 2002]. The near IR study was motivated by the suggestion that photodissociation by excitation of vibrational overtones would significantly increase the overall photolysis rate of HO₂NO₂ [Donaldson *et al.*, 1997]. In light of these new laboratory data, we examine here remote observations of HO₂NO₂ obtained at mid- and high-latitudes and in situ measurements of HO₂ from high-latitude spring.

2. Observations and Model Description

Measurements of HO₂NO₂ were obtained by the JPL MkIV balloon-borne Fourier Transform Infrared spectrometer using solar occultation at 35°N on Sept. 25, 1993 during sunset and at high-latitude (65 to 70°N) on May 8, 1997 during sunrise. Details of these two MkIV flights are given by Sen *et al.* [1998] and Osterman *et al.* [1999], respectively.

Absorption of sunlight by the unresolved Q branch of HO₂NO₂ is apparent in measured spectra near 802.7 cm⁻¹ (Figure 1). The high spectral resolution of MkIV allows this broad absorption feature to be separated from the stronger, narrower absorption lines of O₃, H₂O, and CO₂. Profiles of the volume mixing ratio (vmr) of HO₂NO₂ (Figures 2 and 3) are based on band intensities reported by May and Friedl [1993], which have an estimated accuracy of 20%. Measured profiles of HO₂NO₂ are provided in tabular form in the supplemental material.¹ We also examine in situ measurements of HO₂ obtained by an instrument aboard the ER-2 aircraft near 64°N during spring of 1997 [details given by Wennberg *et al.* 1999].

The photochemical model has been used in many previous studies [e.g., Sen *et al.*, 1998; Osterman *et al.*, 1999]. The abundance of radicals (e.g., NO₂ and HO₂) and reservoir compounds (e.g., HO₂NO₂) are calculated by balancing the production and loss of each species integrated over 24 hours (e.g., diel steady state). For analyses of the MkIV data, abundances of long-lived precursors such as O₃, H₂O, NO_y, and Cl_y are specified from MkIV observations. Profiles of Br_y are based on correlations with N₂O; aerosol surface area is based on zonal, monthly mean profiles from the Stratospheric Aerosol and Gas Experiment II [Sen *et al.*, 1998; Osterman *et al.*, 1999 and references therein]. Constraints for the simulations of these two MkIV flights are provided in tabular form in the supplemental material.¹ The model is similarly constrained by observations of long-lived precursors, aerosol surface area, etc. for analyses of the ER-2 data. These calculations were carried out as described by Wennberg *et al.* [1999], using the constraints given in Table 1 of that paper.

The simulations shown below for both the MkIV and the ER-2 data use three sets of kinetic parameters. The first is based on the most recent evaluation [Sander *et al.*, 2000] and is referred to as the JPL00 model. The second set, denoted Model B, uses several modifications of potential importance for HO₂NO₂: a) the rates for OH + O₃ and HO₂ + O₃ from JPL97 [DeMore *et al.*, 1997] are used because they better

describe the ratio of HO₂ to OH observed in the lower stratosphere and because they are in better agreement with laboratory studies published subsequent to *JPL00* [Lanzendorf *et al.*, 2001]; *b*) the reaction Cl + HNO₄ yielding HCl + NO₂ + O₂ (not considered in the JPL compendia) is included at a rate of 10¹³ cm³ sec⁻¹ [Simonaitis and Leu, 1985]; *c*) UV absorption cross sections for HO₂NO₂ recently measured by Knight *et al.* [2002] are adopted. A third set of calculations uses the same set of kinetic parameters as *Model B*, except photodissociation of HO₂NO₂ in the near IR is added. This calculation, referred to as *Near IR*, uses values for cross sections, quantum yields, and solar flux given in Table 3 of Roehl *et al.* [2002] (note 2).

3. HO₂NO₂ Comparisons

Figures 2 and 3 show comparisons of calculated and observed HO₂NO₂ for the mid-latitude and high-latitude balloon flights, respectively. Calculated profiles found using *JPL00* kinetics exceed observed levels of HO₂NO₂ at mid-latitudes for altitudes between ~20 to 30 km. However, this discrepancy is well within the uncertainty of the calculation, based on considerations such as a factor of 2 uncertainty in the photolysis rate of HO₂NO₂ [DeMore *et al.*, 1997]. For the high-latitude springtime observations, *JPL00* kinetics over estimates the abundance of HO₂NO₂ by as much as a factor of 4. The discrepancy at high-latitude is significant considering uncertainties in both measured and modeled HO₂NO₂.

Uncertainties in NO_x chemistry can not explain the discrepancy between measured HO₂NO₂ at high latitude spring and the *JPL00* simulation. The model simulates observed profiles of NO₂ and NO quite well (differences typically less than 10% for all three sets of kinetic parameters) for both mid-latitudes and high-latitudes, as shown in the supporting material.¹ Revisions to the rates of OH+NO₂+M and OH+HNO₃ in *JPL00* account for earlier discrepancies between modeled and measured NO₂ at both mid- and high-latitudes [Sen *et al.*, 1998; Osterman *et al.*, 1999].

The kinetic parameters adopted for the *Model B* simulation result in lower values of calculated HO₂NO₂ and better agreement with observation. The difference in calculated HO₂NO₂ compared to the *JPL00* simulation is almost entirely due to the change in the rate constants of OH+O₃ and HO₂+O₃. This change lowers modeled HO₂ and increases OH; both of these effects lead to reductions in calculated HO₂NO₂. The rate of the Cl + HO₂NO₂ reaction, included here for completeness, is about a factor of 100 too slow to affect either HO₂NO₂ or HCl. The Knight *et al.* [2002] UV cross sections result in nearly identical photolysis rates of HO₂NO₂ as *JPL00* kinetics for both mid- and high-latitudes: weaker absorption between ~280 to 325 nm using the Knight *et al.* data is compensated by contributions to photolysis longward of 325 nm. The Knight *et al.* measurements do, however, increase our confidence that uncertainties in UV photolysis of HO₂NO₂ can not account for measured HO₂NO₂ at high latitudes.³

Inclusion of near IR photolysis of HO₂NO₂ leads to good agreement between measured and modeled HO₂NO₂ at both mid- and high-latitudes.⁴ Contributions from the near IR dominate photolytic loss of HO₂NO₂ below ~24 km at mid-latitudes and below about ~28 km at high-latitudes. The calculated photolysis rate due to excitation of purely vibrational modes is nearly an order of magnitude larger than estimated by Wennberg *et al.* [1999] because, as discussed by Roehl *et al.* [2002], excitation of the first overtone of OH stretching frequency (near 1.4 μm) was found to have a significant quantum yield for dissociation.

Near IR photolysis has a larger effect at high-latitude spring because of: *a*) strong attenuation of UV light by the high ozone slant column (this lowers the UV contribution to HO₂NO₂ photolysis compared to mid-latitudes); *b*) long days (the IR contribution to HO₂NO₂ photolysis depends essentially on length of sunlight). Calculated contributions to loss of HO₂NO₂ by UV photolysis, near IR photolysis, and reaction with OH are shown in the supplemental material.¹ The fact that near IR photolysis makes the largest contribution to calculated HO₂NO₂ for the region of the atmosphere where standard models (e.g., *JPL00* or *Model B*) most strongly overestimate measured HO₂NO₂ provides compelling evidence for the importance of this mechanism.

4. Implications for HO_x

Figure 4 illustrates the effect of near IR photolysis of HO₂NO₂ on 24 hour average, calculated HO_x. The increase in calculated HO_x is modest (2 to 6%) below ~28 km at mid-latitudes. The increase is dramatic (20 to 60%), however, for high-latitude spring at altitudes below ~28 km. The perturbation extends into the upper troposphere (UT) for both regions and is large (50 to 60%) in the UT at high-latitudes.

Changes in calculated HO_x are largest for high latitude spring below ~28 km for the same reasons described above (weaker UV and longer days result in a stronger perturbation to HO₂NO₂) plus the presence of characteristically high levels of NO_x [e.g., Osterman *et al.*, 1999]. The loss of HO_x by (1)-(2) is catalyzed by NO_x; for the *JPL00* simulation, this cycle plays a stronger role in HO_x photochemistry at high-latitude spring compared to mid-latitudes. The effect of near IR HO₂NO₂ photolysis on calculated HO_x depends, therefore, on ambient NO_x. This dependence is important for assessing the tropospheric implications of this process.

The influence of near IR photolysis of HO₂NO₂ on HO_x is further illustrated in Figure 5, which compares modeled and measured HO₂ in the lower stratosphere near 64°N during spring. The *JPL00* simulation significantly underestimates measured HO₂ throughout the day. An important change in the *JPL00* kinetic parameters, relative to *JPL97*, is a reduction in the reaction probability (γ) for BrONO₂ hydrolysis from 0.8 to ~0.2 for the temperature and humidity of these observations. This change reduces the morning rise of HO₂ due to photolysis of HOBr that was apparent in the *JPL97* simulation of Wennberg *et al.* [1999]. Adopting the *Model B* kinetic parameters results in a slight increase in calculated HO₂. Allowing for the near IR photolysis of HO₂NO₂ leads to a ~20% increase in 24 hr average HO₂ and better agreement with the observed rise of HO₂ in early morning due to the rapid photolysis of HO₂NO₂ at high solar zenith angles. Nonetheless, measured HO₂ and OH (figure shown in supplemental material¹) are still underestimated by this model.

The discrepancy between measured HO₂ and OH and the *Near IR* model calculation is not significant given the estimated possible 30% systematic error in the HO_x measurements [Wennberg *et al.*, 1999] (figure shown in supplemental material¹). However, the precision of the HO_x data is much better; e.g., any systematic error will not vary with solar zenith angle (SZA). The shapes of HO₂ vs. SZA and OH vs. SZA from the *Near IR* simulation agree well with observed SZA dependencies. The discrepancy between

measured and modeled HO_x for the *JPL00* and *Model B* simulations is significant because the measured shape of HO_x vs. SZA differs considerably from the model calculations.

Nonetheless, it is interesting to speculate on possible reasons for the shortfall between calculated HO_x from the *Near IR* simulation and the HO_x observations (assuming the HO_x calibration is correct). It is unlikely that this shortfall can be entirely due to errors in the photolysis rate of HO₂NO₂. Sensitivity studies (not shown) indicate the integrated burst of HO_x during morning supplied by photolysis of HO₂NO₂ is limited once photolysis becomes the dominant sink of HO₂NO₂ (e.g., the concentration of HO₂NO₂ becomes inversely proportional to its photolysis rate). If the rate of OH+HO₂NO₂ is reduced to its lower limit, then calculated HO_x within the *Near IR* simulation lies close to the observations (not shown). Similarly, if this reaction does not yield H₂O with 100% efficiency, model and measured HO_x are in better agreement.

Another possible explanation of the measured HO_x is that γ of BrONO₂ hydrolysis, for conditions of these observations, is considerably faster than 0.2. The *JPL00* recommendation for BrONO₂ hydrolysis is based on laboratory results extrapolated to water activity levels of the lower stratosphere [D. Hanson, submitted manuscript, 2002]. The model simulation labeled " $\gamma=0.8$ " in Figure 5 shows that the observed, integrated morning burst of HO₂ might be supplied by photolysis of both HO₂NO₂ and HOBr. The slight difference between the timing of the measured morning rise of HO₂ and the $\gamma=0.8$ simulation could be indicative of errors in the calculated actinic flux, errors in the photolysis rate of HOBr and/or HO₂NO₂, or supply of HO_x from some other precursor. The good agreement between the modeled and measured early morning rise of NO, illustrated in the supplemental material¹, suggests the actinic flux calculation is carried out correctly [Gao *et al.*, 2001]. Calculations shown in the supplemental material¹ indicate that BrONO₂ hydrolysis, in the absence of near IR photolysis of HO₂NO₂, is unable to account for the observed fall off of HO₂ with increasing SZA in the evening regardless of assumptions regarding γ or Br_y.

5. Concluding Remarks

Near IR photolysis of HO₂NO₂, first suggested by Donaldson *et al.* [1997], alters the coupling between NO_x and HO_x in stratospheric and upper tropospheric photochemical models. In the lower stratosphere, HO_x radicals are the dominant sink for photochemical loss of O₃. The increased levels of HO_x suggested by this analysis will likely result in greater sensitivity of calculated O₃ to perturbations such as increases in stratospheric H₂O. In the upper troposphere (UT), production of ozone via oxidation of carbon monoxide and other hydrocarbons proceeds via coupled HO_x:NO_x photochemistry [Folkins *et al.*, 1997]. The efficiency of this chemistry is thought to become limited at moderate concentrations of NO_x due to loss of HO_x by reactions (1) and (2) [e.g., Jaeglé *et al.*, 2001]. The reduced efficiency of this sink implies that production of ozone in the UT will be positively correlated with the abundance of NO to higher levels of NO_x than is found in many models.

We conclude by noting that space-borne observations of HO₂NO₂ can provide significant advances in constraints on the photochemistry of the upper troposphere and lower stratosphere. Measurements of HO₂NO₂ co-located with observations of NO₂ provide a means to determine concentrations of HO₂. Near IR photolysis reduces the lifetime of HO₂NO₂, simplifying the

interpretation of observations. There is hope that observations of HO₂NO₂ will become available in the near future, since it is measured by the Michelson Interferometer for Passive Atmospheric Sounding instrument aboard the ESA ENVISAT spacecraft and is a "special product" of the Tropospheric Emission Spectrometer to be launched on the NASA Aura spacecraft.

Acknowledgments. We thank Gary Knight and Coleen Roehl for making available measurements of HO₂NO₂ cross sections prior to publication and the anonymous reviewers for helpful comments. This work was funded by the NASA Upper Atmosphere Research, Atmospheric Chemistry Modeling and Analysis, and Atmospheric Effects of Aviation Programs. Research at the Jet Propulsion Laboratory, California Institute of Technology, is performed under contract with the National Aeronautics and Space Administration.

Notes

1. Supporting material is available via Web browser or anonymous FTP from <ftp://kosmos.agu.org>, directory "apend"; subdirectories in the ftp site are arranged by paper number. Information on electronic supplements is at http://www.agu.org/pubs/esupp_about.html.

2. We consider Rayleigh scattering and assume no other attenuation of incident solar radiation in the near IR, except for an ozone cross section of 2.76×10^{-22} cm² at 763 nm, the spectral region of the 4v₁ band of HO₂NO₂.

3. DeMore *et al.* [1997] give a factor of 2 uncertainty for the photolysis rate of HO₂NO₂. The uncertainty estimates of Knight *et al.* [2002] are 10 to 15% for $\lambda < 320$ nm. However, the Knight *et al.* cross sections for stratospheric conditions are based on an extrapolation to lower temperatures than the laboratory experiment.

4. An estimate of the uncertainty in calculated HO₂NO₂, for the kinetic parameter of the *Near IR* simulation, is given in Figures 2 and 3. This estimate was computed by varying each of the kinetic parameters that control production or loss of HO₂NO₂ by their estimated uncertainty, calculating the effect on HO₂NO₂, and combining effects from each parameter in a root-sum-squares fashion. The estimated uncertainties are from DeMore *et al.* [1997] and Knight *et al.* [2002].

References

- DeMore, W. B., *et al.*, Chemical kinetics and photochemical data for use in stratospheric modeling, Evaluation No. 12, *JPL Publication 97-4*, Jet Propulsion Laboratory, 1997.
- Donaldson, D. J., *et al.*, Atmospheric radical production by excitation of vibrational overtones via absorption of visible light, *Geophys. Res. Lett.*, 24, 2651-2654, 1997.
- Folkins, I., *et al.*, OH, HO₂, and NO in two biomass burning plumes: Sources of HO_x and implications for ozone production, *Geophys. Res. Lett.*, 24, 3185-3188, 1997.
- Gao, R. S. *et al.*, J_{NO2} at high solar zenith angles in the lower stratosphere, *Geophys. Res. Lett.*, 28, 2405-2408, 2001.

- Jaeglé L., D. J. Jacob, W. H. Brune, and P. O. Wennberg, Chemistry of HO_x radicals in the upper troposphere, *Atmos. Environ.*, *35*, 469-489, 2001.
- Knight, G., A. R. Ravishankara, and J. B. Burkholder, UV absorption cross sections of HO₂NO₂ between 343 and 273 K, *J. Phys. Chem. A.*, submitted, 2002.
- Lanzendorf E. J., *et al.*, Comparing atmospheric [HO₂]/[OH] to modeled [HO₂]/[OH]: Identifying discrepancies with reaction rates, *Geophys. Res. Lett.*, *28*, 967-970, 2001.
- May, R. D. and R. R. Friedl, Integrated band intensities of HO₂NO₂ at 220 K, *J. Quant. Spect. Rad. Trans.*, *50*, 257-266, 1993.
- Osterman, G.B., *et al.*, Partitioning of NO_y species in the summer Arctic stratosphere, *Geophys. Res. Lett.*, *26*, 1157-1160, 1999.
- Rinsland, C. P., *et al.*, Evidence for the presence of the 802.7 cm⁻¹ band Q branch of HO₂NO₂ in high resolution solar absorption spectra of the stratosphere, *Geophys. Res. Lett.*, *13*, 761-764, 1986.
- Roehl, C. A., *et al.*, Photodissociation of HNO₄ in the near IR., *J. Phys. Chem. A.*, *106*, 3766-3772, 2002.
- Sander, S. P., *et al.*, Chemical kinetics and photochemical data for use in stratospheric modeling, Evaluation No. 13, *JPL Publication 00-3*, Jet Propulsion Laboratory, 2000.
- Sen, B., *et al.*, Measurements of reactive nitrogen in the stratosphere, *J. Geophys. Res.*, *103*, 3571-3585, 1998.
- Simonaitis, R. and M. T. Leu, Rate constant for the reaction Cl+HO₂NO₂→Products, *Int. J. Chem. Kin.*, *17*, 293-301, 1985.
- Wennberg, P. O., *et al.*, Twilight observations suggest unknown sources of HO_x, *Geophys. Res. Lett.*, *26*, 1373-1376, 1999.

R. J. Salawitch, G. C. Toon, B. Sen, J.-F. Blavier, JPL, Mail Stop 183-601, 4800 Oak Grove Drive, Pasadena, CA 91109.
P. O. Wennberg, MS 150-21, Caltech, Pasadena, CA, 91125.

(Received 27 February 2002; revised 15 April 2002; accepted 9 May 2002.)

AGU Copyright:

Copyright 2002 by the American Geophysical Union.

Paper number 2002GL015006R.
0094-8276/02/2002GL015006R\$05.00

Published in 2002 by the American Geophysical Union.

Figure 1. *Bottom Panel:* Measured transmittance (diamonds connected by black lines) for a MkIV spectrum obtained on May 8, 1997 with a tangent altitude of 10.4 km. The estimated contribution of the unresolved Q branch of HO₂NO₂ to the transmittance is shown (red line). Contributions from other species are also shown, as indicated. *Top Panel:* Calculated residuals to the measured transmittance found by the retrieval algorithm, allowing for absorption by HO₂NO₂ (black line) and neglecting absorption by HO₂NO₂ (red line).

Figure 2. Profile of HO₂NO₂ measured by MkIV on Sept. 25, 1993 at 35°N (points w/ error bars) compared to model simulations for three sets of kinetic parameters: 1) *JPL00*; 2) *Model B* (see text); 3) *Near IR* photolysis of HO₂NO₂ plus *Model*

B. Error bars for observed HO₂NO₂ represent 1σ precision. The 1σ uncertainty in calculated HO₂NO₂ for the *Near IR* model, based on uncertainties in rate constants of its formation and loss processes, is shown by the error bars bounded by vertical line segments.

Figure 3. Same as Figure 2, for May 8, 1997 at 65 to 70°N.

Figure 4. Calculated change in 24 hour average HO_x (OH+HO₂) when near IR photolysis is added to a simulation based on *Model B* kinetics (solid line) and to a simulation based on *JPL00* kinetics (dashed line).

Figure 5. Observations of HO₂ obtained on the morning of April 30, 1997 and the afternoon of May 9, 1997 from the ER-2 aircraft near 64°N in the lower stratosphere compared to model simulations using the three sets of kinetic parameters described in Figure 2. A fourth simulation, allowing for a reaction probability of 0.8 for BrONO₂ hydrolysis within the *Near IR* model, is also shown.

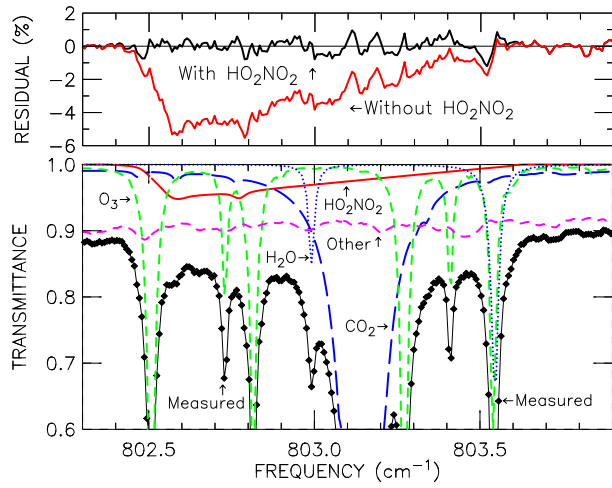


Figure 1

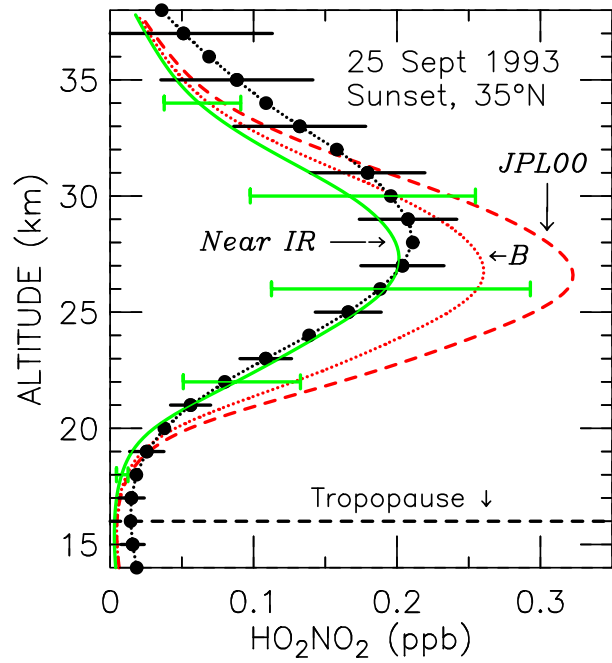


Figure 2

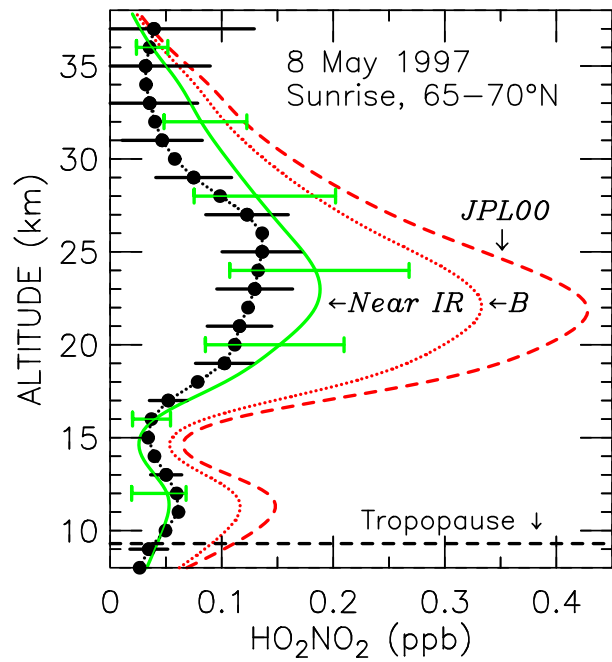


Figure 3

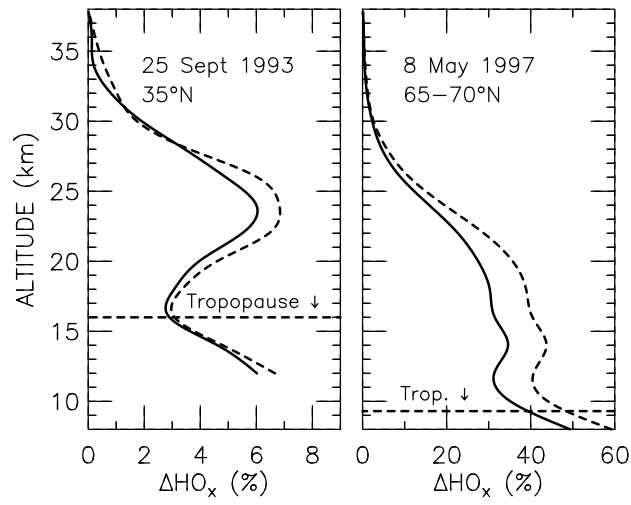


Figure 4

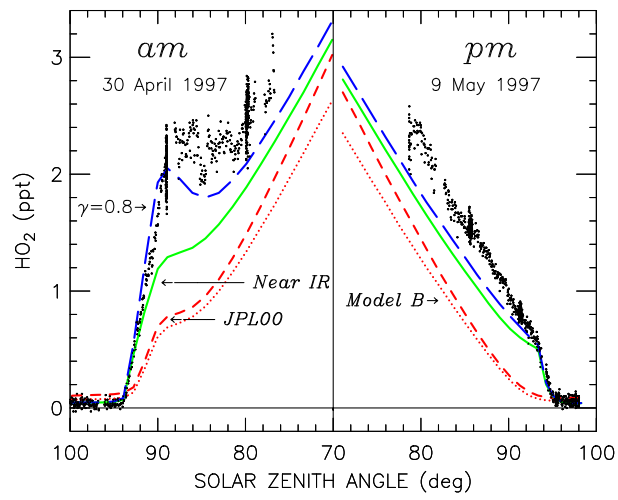


Figure 5

Supplemental Material for Salawitch *et al.*, Near IR Photolysis of HO₂NO₂ Manuscript 2002GL015006

Observations and Model Inputs

MkIV measurements of the volume mixing ratio (vmr) of HO₂NO₂ at 35°N, sunset on Sept. 25, 1993 are given in Table 1. Measurements of HO₂NO₂ made between ~65 and 70°N, sunrise on May 8, 1997 are listed in Table 2. The uncertainties given in the tables are 1σ estimates of the measurement precision. Uncertainty in the HO₂NO₂ line strengths is estimated to be 20% [May and Friedl, 1993]; this is the dominant contribution to the systematic error of the HO₂NO₂ measurement.

Model inputs for the simulations are given in Tables 3 and 4. The albedos were obtained from Total Ozone Mapping Spectrometer reflectivity data (raw data at <ftp://jwocky.gsfc.nasa.gov>) for the time and place of observation. Profiles of sulfate aerosol surface area (“Surf. Area”) were obtained from monthly, zonal mean profiles measured by SAGE II [Thomason *et al.*, 1997 updated via private communication]. The profile of Br_y is based on the Wamsley *et al.* [1998] relation with N₂O, using MkIV measurements of N₂O. All other model inputs given in Tables 3 and 4 are based on direct MkIV measurements [see Sen *et al.*, 1998 and Osterman *et al.*, 1999 for details]. Finally, we note the latitude of the MkIV tangent point varied considerably during sunrise on May 8, 1997. The simulations shown here were obtained using different latitudes for each altitude, as indicated in Table 4.

Additional Model – Measurement Comparisons

A few additional comparisons of calculated and observed species are given here to support the conclusions of the paper. Figure 6 shows calculated HO₂NO₂ loss frequencies (averaged over 24 hours) due to photolysis in the UV, photolysis in the near IR, and reaction with OH (results for reaction with OH are shown for the *JPL00* and *Near IR* model runs, since calculated concentrations of OH vary considerably depending on kinetic parameters). The longer days at high-latitude during spring, coupled with lower abundances of OH and lower rates of UV photolysis (due to higher slant column abundances of O₃), result in near IR photolysis having a much more pronounced effect on total loss of HO₂NO₂ for the May 1997 simulation than for the Sept 1993 model run.

Figure 7 shows that observed profiles of NO₂ are simulated accurately for both mid-latitudes and high-latitude spring. Revisions to the rate of OH+NO₂+M in the *JPL00* compendium resolve the discrepancies discussed by Sen *et al.* [1998] and Osterman *et al.* [1999]. Most importantly, the accurate simulations of observed NO₂ demonstrate that uncertainties in NO_x photochemistry can not explain the factor of 4 overestimate of HO₂NO₂ at high-latitude springtime by the *JPL00* model run.

The comparison of measured OH and the four model simulations shown in Figure 8 looks similar to the HO₂ comparisons shown in our paper. This figure is included here to illustrate that neither the *JPL00* nor the *Model B* simulation matches the observed shape of OH versus solar zenith angle. Thus, the discrepancy discussed in the paper is for HO_x (OH+HO₂) and can not be accounted for by errors in the simulation of the OH to HO₂ ratio.

The comparisons of modeled and measured HO₂ shown in Figure 9 are provided to support the statement in our paper that BrONO₂ hydrolysis, in the absence of near IR

photolysis of HO₂NO₂, can not account for the observed shape of HO₂ vs SZA near evening twilight. The model shown by the solid green curve in Figure 9 assumes a reaction probability of 0.8 for BrONO₂ hydrolysis (considerably faster than expected for these conditions [D. Hanson, submitted manuscript, 2002]) as well as 20 pptv of Br_y (nearly a factor of two higher than our estimate of Br_y based on published relations with N₂O [e.g., Table 1 of Wennberg *et al.*, 1999]). Even with these assumptions, the measured shape of HO₂ vs SZA is considerably different than the calculated shape.

The comparisons of measured and modeled NO₂ and NO shown in Figure 10 suggest the actinic flux calculation is carried out correctly [Gao *et al.*, 2001]. For these simulations, the model is perturbed slightly to assure good agreement with measured NO_x (NO + NO₂) [Wennberg *et al.*, 1999]. This perturbation is carried out to assure proper model representation of the OH/HO₂ ratio. This is particularly important for simulations of HO_x due to the autocatalytic nature of some of the HO_x loss processes [e.g., Wennberg *et al.*, 1999].

The final illustration, Figure 11, is identical to Figure 5 of the published paper except the measurements of HO₂ have been reduced by 30% (the potential systematic error of the HO_x observations may be this large [Wennberg *et al.*, 1999]). This figure is included here to support our conclusion that the *Near IR* model reproduces the overall shape of observed HO₂ throughout the day, whereas the *JPL00* and *Model B* simulations are not in agreement with this measured shape.

References for Supplemental Material

- DeMore, W. B., *et al.*, Chemical kinetics and photochemical data for use in stratospheric modeling, Evaluation No. 12, *JPL Publication 97-4*, Jet Propulsion Lab., Pasadena, CA, 1997.
- Gao, R. S., *et al.*, J_{NO₂} at high solar zenith angles in the lower stratosphere, *Geophys. Res. Lett.*, 28, 2405-2408, 2001.
- May, R. D. and R. R. Friedl, Integrated band intensities of HO₂NO₂ at 220 K, *J. Quant. Spect. Rad. Trans.*, 50, 257-266, 1993.
- Osterman, G. B., *et al.*, Partitioning of NO_y species in the summer Arctic stratosphere, *Geophys. Res. Lett.*, 26, 1157-1160, 1999.
- Roehl, C. A., *et al.*, Photodissociation of peroxyoxynitric acid in the near-IR, *J. Phys. Chem. A*, 106, 3766-3772, 2002.
- Sen, B., *et al.*, Measurements of reactive nitrogen in the stratosphere, *J. Geophys. Res.*, 103, 3571-3585, 1998.
- Sander, S. P., *et al.*, Chemical kinetics and photochemical data for use in stratospheric modeling, Evaluation No. 13, *JPL Publication 00-3*, Jet Propulsion Lab., Pasadena, CA, 2000.
- Thomason, L. W., L. R. Poole, and T. Deshler, A global climatology of stratospheric aerosol surface area density deduced from Stratospheric Aerosol and Gas Experiment II measurements: 1984-1994, *J. Geophys. Res.*, 102, 8967-8976, 1997.
- Wamsley, P. R., *et al.*, Distribution of H-1211 in the upper troposphere and lower stratosphere and the 1994 bromine budget, *J. Geophys. Res.*, 103, 5313-1526, 1998.
- Wennberg, P. O., *et al.*, Twilight observations suggest unknown sources of HO_x, *Geophys. Res. Lett.*, 26, 1373-1376, 1999.

Table 1. MkIV Measurements of HO₂NO₂, Sept. 25, 1993, Sunset.

Altitude	VMR (pptv)	VMR Uncertainty (pptv)
14.	18.48	8.5
15.	15.71	8.1
16.	14.27	8.4
17.	14.81	9.0
18.	18.27	10.
19.	25.52	12.
20.	37.78	13.
21.	56.10	14.
22.	79.94	16.
23.	108.5	18.
24.	138.7	21.
25.	166.0	23.
26.	188.3	26.
27.	203.8	29.
28.	211.0	32.
29.	207.7	34.
30.	195.7	37.
31.	179.5	40.
32.	158.0	43.
33.	132.2	46.
34.	108.7	49.
35.	88.36	53.
36.	68.97	58.
37.	51.13	62.
38.	35.91	69.

Table 2. MkIV Measurements of HO₂NO₂, May 8, 1997, Sunrise.

Altitude	VMR (pptv)	VMR Uncertainty (pptv)
8.	26.45	32.
9.	34.69	17.
10.	49.62	14.
11.	61.26	16.
12.	59.63	15.
13.	50.25	14.
14.	39.70	14.
15.	34.06	14.
16.	36.99	15.
17.	52.13	17.
18.	78.44	22.
19.	102.5	26.
20.	111.7	28.
21.	116.0	29.
22.	123.6	32.
23.	129.6	34.
24.	132.6	35.
25.	136.3	36.
26.	136.3	38.
27.	122.7	37.
28.	98.53	35.
29.	74.89	34.
30.	57.92	34.
31.	46.64	36.
32.	40.18	39.
33.	35.50	43.
34.	32.14	48.
35.	31.77	58.
36.	35.34	73.
37.	39.25	90.
38.	42.18	110.

Table 3. Model Inputs for Sept. 25, 1993, Sunset.^a

Z (km)	T (K)	p (mbar)	O ₃ (ppmv)	H ₂ O (ppmv)	CH ₄ (ppmv)	NO _y (ppbv)	Cl _y (ppbv)	Br _y (pptv)	CO (ppbv)	Surf. Area ($\mu\text{m}^2/\text{cm}^3$)
12.	225.0	210.5	0.037	17.96	1.66	0.368	0.001	0.01	67.7	1.44
14.	211.6	154.1	0.047	7.24	1.72	0.217	0.001	0.01	65.2	1.79
16.	200.0	110.4	0.124	6.08	1.67	0.290	0.100	0.01	43.9	3.64
18.	202.3	78.75	0.437	4.99	1.61	1.09	0.201	3.39	22.6	6.50
20.	209.1	56.57	1.28	4.03	1.48	3.57	0.871	8.34	13.2	5.77
22.	215.6	41.13	2.77	4.62	1.18	8.02	1.929	14.6	11.8	2.88
24.	219.3	30.13	4.50	4.83	1.09	10.2	2.47	15.5	12.7	1.18
26.	222.4	22.16	6.31	4.79	1.09	11.8	2.72	15.7	14.3	0.65
28.	224.5	16.37	7.60	4.88	1.05	14.3	2.94	15.9	16.2	0.45
30.	227.9	12.14	8.27	5.18	0.955	16.7	3.15	16.0	16.0	0.26
32.	230.5	9.047	8.26	5.46	0.876	17.8	3.29	16.0	15.1	0.13
34.	230.4	6.742	8.10	5.45	0.809	18.3	3.31	16.0	16.4	0.066
36.	240.0	5.060	7.97	5.67	0.687	17.6	3.41	16.0	19.0	0.035
38.	242.2	3.826	7.41	5.84	0.660	17.3	3.35	16.0	23.7	0.022

^a Latitude = 34.5°N; Solar Declination = -1.1°; Albedo = 0.46**Table 4.** Model Inputs for May 8, 1997, Sunrise.^a

Z (km)	T (K)	p (mbar)	O ₃ (ppmv)	H ₂ O (ppmv)	CH ₄ (ppmv)	NO _y (ppbv)	Cl _y (ppbv)	Br _y (pptv)	CO (ppbv)	Surf. Area ($\mu\text{m}^2/\text{cm}^3$)	Lat. (°N)	Albedo
8.	226.9	345.4	0.104	27.80	1.77	0.79	0.005	0.01	89.4	1.54	70.47	0.85
10.	222.5	254.1	0.440	10.10	1.65	2.20	0.447	3.51	37.2	2.45	70.02	0.77
12.	231.1	188.4	0.717	3.02	1.58	3.30	0.718	5.31	20.5	1.52	69.66	0.72
14.	231.0	140.2	0.509	3.09	1.65	1.95	0.356	2.44	27.1	0.957	69.35	0.66
16.	229.3	104.4	0.860	3.51	1.60	2.65	0.662	4.72	18.3	0.944	69.08	0.59
18.	228.2	77.44	2.03	4.59	1.38	6.05	1.58	11.4	12.1	0.900	68.81	0.53
20.	228.8	57.52	2.95	4.82	1.32	8.46	2.10	13.0	12.2	0.706	68.56	0.46
22.	228.6	42.73	3.73	4.89	1.28	9.76	2.28	13.9	13.3	0.480	68.29	0.40
24.	228.5	31.74	4.02	5.13	1.17	12.50	2.86	15.6	14.7	0.287	68.03	0.35
26.	228.9	23.58	4.20	5.44	0.994	15.10	3.16	16.0	15.2	0.173	67.76	0.31
28.	229.6	17.54	4.48	5.76	0.875	16.70	3.46	16.0	15.9	0.102	67.48	0.28
30.	230.8	13.06	4.86	6.07	0.767	17.20	3.50	16.0	15.7	0.061	67.19	0.25
32.	233.2	9.749	5.29	6.25	0.651	16.00	3.53	16.0	16.5	0.035	66.85	0.18
34.	236.0	7.299	6.05	6.34	0.583	14.80	3.41	16.0	18.4	0.023	66.47	0.11
36.	241.3	5.502	6.43	6.42	0.512	13.30	3.21	16.0	18.8	0.018	65.99	0.11
38.	247.4	4.171	6.61	6.64	0.376	10.80	2.91	16.0	19.8	0.014	64.88	0.08

^a Solar Declination = 17.2°. Latitude and Albedo specified, as indicated, for each altitude.

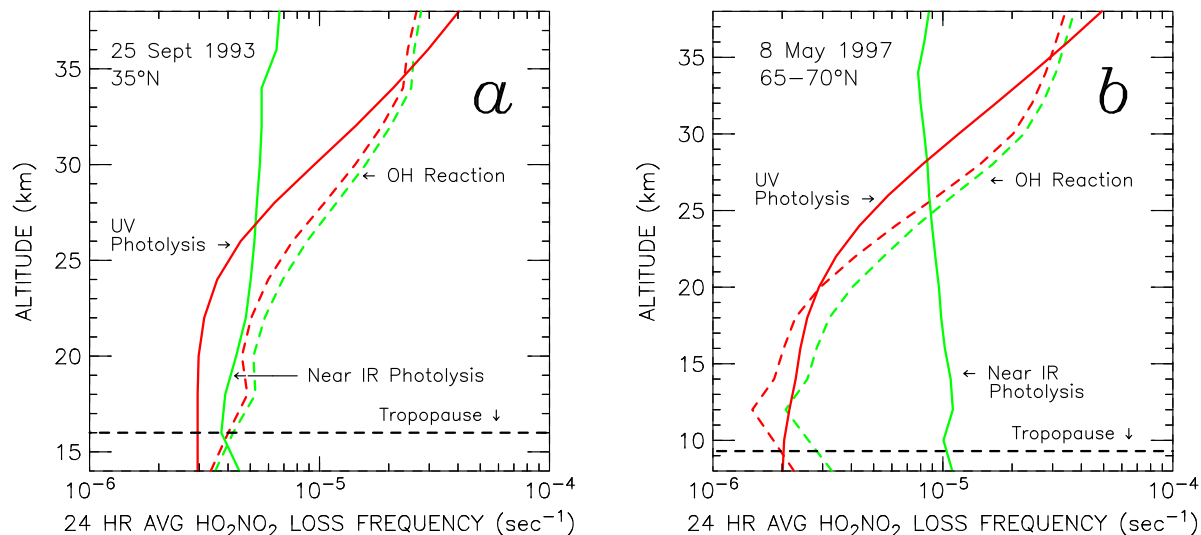


Figure 6. Panel *a*. Calculated loss frequencies of HO_2NO_2 for the Sept. 25, 1993 simulation, averaged over 24 hours, due to UV photolysis only using *JPL00* [Sander *et al.*, 2000] cross sections (red solid), due to near IR photolysis only using cross sections of *Roehl et al.* [2002] (green solid), and due to reaction of OH with HO_2NO_2 (red dashed for *JPL00* kinetics; green dashed for *Near IR* kinetics). Other sinks of HO_2NO_2 , such as thermal decomposition and reaction with atomic Cl, are considered in the model but do not contribute appreciably to the loss of HO_2NO_2 . Panel *b*. Same as *a*, for the May 8, 1997 simulation.

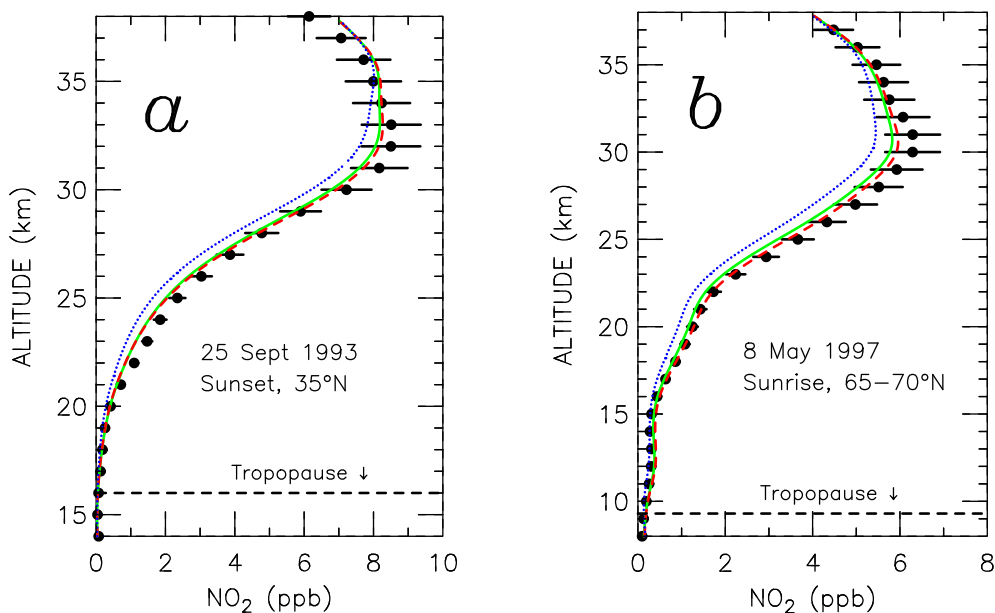


Figure 7. Panel *a*. Profile of NO_2 measured by MkIV on Sept. 25, 1993 at sunset compared to model simulations for *JPL00* kinetics (red dashed line) and *Near IR* kinetics (green solid line). Also shown, for comparison to earlier published results, is a model result using *JPL97* [DeMore *et al.*, 1997] kinetics (dotted blue line). Results from the *Model B* simulation (not shown) are nearly identical to those from the *JPL00* model run. Error bars on the data denote 1σ measurement precision. Panel *b*. Same as *a*, for May 8, 1997 at sunrise.

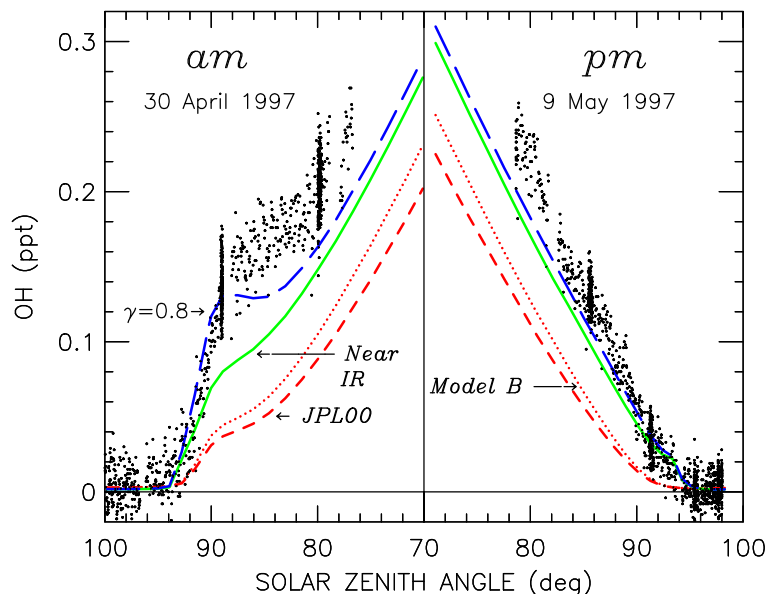


Figure 8. Observations of OH obtained on the morning of April 30, 1997 and the afternoon of April 30, 1997 and the afternoon of May 9, 1997 from the ER-2 aircraft compared to model simulations for four sets of kinetic parameters: 1) *JPL00*; 2) *Model B* (see text); 3) *Near IR* photolysis of HO_2NO_2 plus *Model B*; 4) allowing for a reaction probability of 0.8 for BrONO_2 hydrolysis within the *Near IR* model.

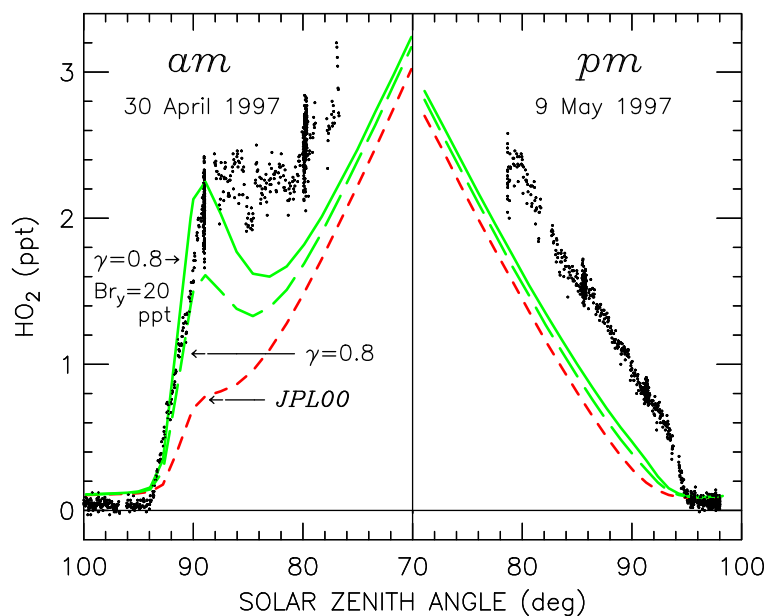


Figure 9. Observations of HO_2 obtained on the morning of April 30, 1997 and the afternoon of May 9, 1997 from the ER-2 aircraft compared to model simulations for three sets of kinetic parameters: 1) *JPL00*; 2) allowing for a reaction probability of 0.8 for BrONO_2 hydrolysis within the *JPL00* model; 3) allowing for a reaction probability of 0.8 for BrONO_2 hydrolysis within the *JPL00* model plus raising the level of Br_y from 12.9 pptv [Wennberg *et al.*, 1999] to 20 pptv.

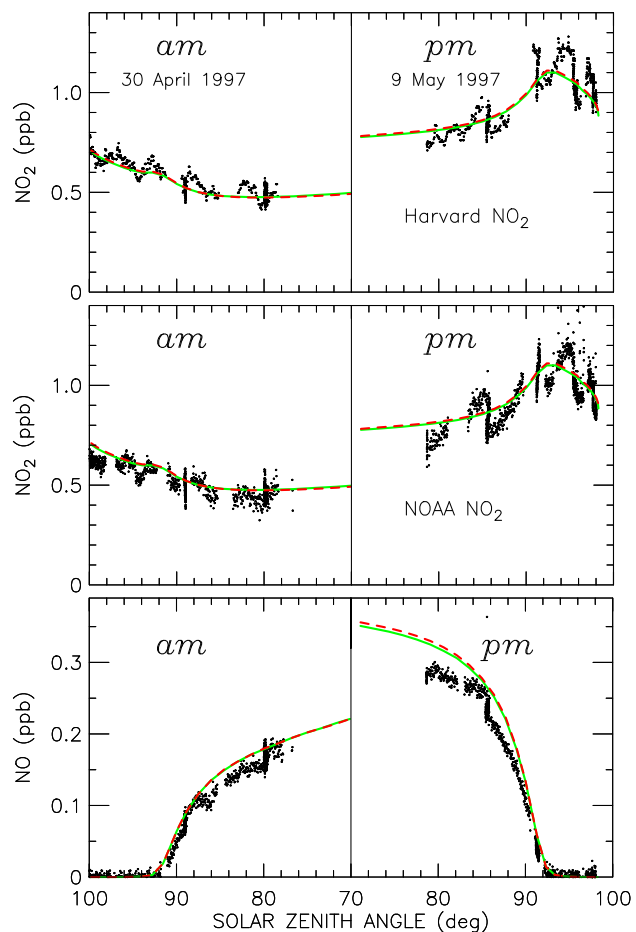


Figure 10. Observations of NO_2 and NO obtained on the morning of April 30, 1997 and the afternoon of May 9, 1997 from the ER-2 aircraft compared to model simulations for *JPL00* kinetics (red dashed line) and *Near IR* kinetics (green solid line). Results from the other simulations (not shown) are nearly identical to those shown. The data are described by *Gao et al.* [2001] and references therein.

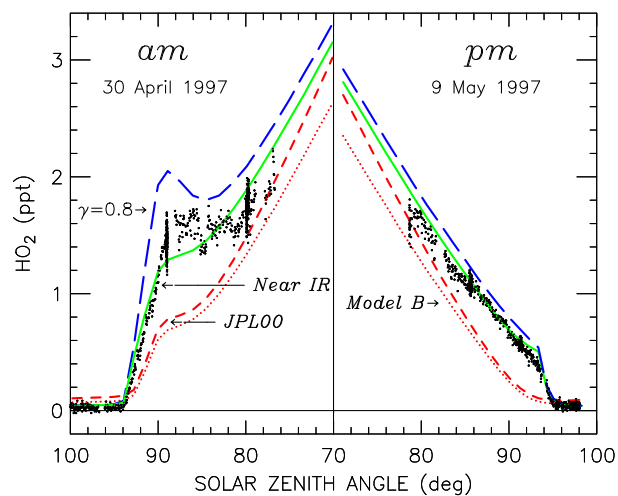


Figure 11. Same as Figure 5 of our paper, except the observations of HO_2 have been lowered by 30%, which corresponds to the potential systematic error that could be present in the observations.